Indian Journal of Advances in Chemical Science

Article

Preparation and Characterization of Tin (IV) Oxide - Silica Nanocomposite Synthesized from Rice Husk Ash

Aung Phyo Kywae[1], Khant Nyar Oo[2], Moe Moe Aye[3], Hla Hla Soe[3], Hlaing Hlaing Myint[3]*

[1]Department of Chemistry, Shwebo University, Shwebo, Myanmar, 02231, [2]Department of Chemistry, Meiktila University, Mandalay, Myanmar, 05181, [3]Department of Chemistry, Monywa Unive rsity, Monywa, Myanmar, 02301

ABSTRACT

Rice husk (RH) and RH ash (RHA) are good sources of low-cost adsorbents. This work presented the results of the study on preparation and characterization of tin oxide – silica nanocomposite synthesized from RHA using sol gel method. Nanosilica (SiO_2) was extracted by calcination of HCl treated RHA at 700°C for 6 h. The physicochemical properties SiO_2, SnO_2 and their nanocomposite (SnO_2–SiO_2) were characterized by scanning electron microscopy, Fourier transform infrared spectroscopy, X-ray diffraction spectrometer, and UV-Vis spectrophotometer (UV). Surface areas and crystallite size of SiO_2, SnO_2 and their nanocomposite (SnO_2–SiO_2) were calculated using Sear's method and Debye Scherrer equation. Characteristic results revealed that SiO_2, SnO_2, and their nanocomposite (SnO_2–SiO_2) were successfully synthesized from RHA. Thus, the synthesized nanosilica SiO_2, SnO_2, and their nanocomposite (SnO_2–SiO_2) can be used for application in dye degradation of wastewater treatments with recyclable nanocomposite.

Key words: Nanosilica, Tin-oxide nanocomposite, Rice husk ash, Calcination, Sol gel method.

1. INTRODUCTION

Agroindustry has generated a large content of residues and the necessity of utilization of these residues might reduce pollution and increase energy savings. Among these residues, rice husks (RH) have received attention due to its large volume produced and high content of amorphous silica [1,2]. Myanmar has a large agricultural potential such as RH that can support economic activity. For example, RH has been used to produce silica as a raw material for biosorbents [3]. Waste RH is being very abundant in Myanmar, an agricultural country. Nanosilica has now applied in various fields including science and industry [4]. Recently, mesoporous SiO_2 has been proved to be an extensively significant new kind of functional material with regular channels, large surface area, high thermal stability, and tunable pore sizes over a wide range. It is used in different fields such as catalysis, functional materials, and nanodevices sorption and energy storage [5]. SiO_2 nanosilica presents unique properties, such as mechanical, catalytic, magnetic, and optical properties, which lead them to be used in paints, plastic, ceramics, batteries, and cosmetics. Moreover, silica has been widely used as catalysts and various kinds of organic-inorganic composite materials [6]. Tin (IV) oxide nanoparticle (NP) is industrially an important semiconductor, because of low thermal stability and aggregation, which can be overcome by incorporating amorphous silica to form SnO_2-SiO_2 nanocomposite [7]. Due to their semiconductor, electronic, optical, and catalytic properties, SnO_2 NPs can be used in a variety of applications in industry, such as solar cells, photo catalysis, and sensors [8]. Silicates containing tin have attracted much attention due to their surface acidity and catalytic activity in a variety of reactions [9]. Burning agricultural residue has also been one of the most effective adsorbents in removing dye from contaminated wastewater. The utilization of abundant natural materials and certain waste products from industrial or agricultural operations as low-cost adsorbents for the removal of dyes is a sustainable approach [10]. Tin (IV) oxide (SnO_2) was synthesized using the Sol gel method. The preparation of SiO_2 using RH ash biomass (RHA) has been developed for adsorption of some dyes and wastewater treatment [11]. However, it is a big challenge to use new materials, especially amorphous silica from Myanmar biomass for preparation of SiO_2. Silica from RHA can be obtained easily and at a relatively low cost by the extraction process. The extraction process is affected by several factors such as solvent concentration and the ratio of the solvent to the RHA [12,13]. Since silica can be produced from RHA, several reports have addressed the extraction of silica from RH. In this research, the synthesis and characterization of the SiO_2, SnO_2, and SnO_2–SiO_2 nanocomposite. This research was divided into two phases: There are one phase was preparation SiO_2 from RH, SnO_2 and SnO_2–SiO_2 nanocomposite. Second phase was characterizations of SiO_2, SnO_2, and SnO_2–SiO_2 nanocomposite were analyzed by using scanning electron microscopy (SEM), Fourier transform infrared spectroscopy (FTIR), X-ray diffraction (XRD) and UV-Vis spectrophotometer. Surface areas and crystallite size of SiO_2, SnO_2, and SnO_2–SiO_2 nanocomposite were calculated using sear's method in equations (1) and Debye Scherrer equation (2) (Sears, 1956), (Scherrer, 1918), (Langford and Wilson, 1978) [14-16]. The use of RHA in the composite can provide several advantages such as increased strength and endurance, reduce the cost of materials, reducing the environmental impact of waste materials, and reduce

***Corresponding author:**
Hlaing Hlaing Myint,
E-mail: hlainghlaingmyint80@gmail.com

ISSN NO: 2320-0898 (p); 2320-0928 (e)
DOI: 10.22607/IJACS.2023.1101002

Received: 08th December 2022;
Revised: 21th December 2022;
Accepted: 25th December 2022

CO_2 emissions. This process not only produces valuable silica but also reduces pollution problems caused by the uncontrolled combustion of RH [17]. Finally, this research can be applied for possible application of technological applications.

2. EXPERIMENTAL

2.1. Preparation of RHA and Extraction of Silica (SiO_2) from RHA

The RH was washed with double distilled (DD) water and filtered, and then treated with 0.001 M HCl in 1: 3 (RH: acid) ratio for approximately 24 h. After that RH was filtered and washed with DD water to a pH of 7. The filtered RH was calcinated in a muffle furnace at 600°C for 4 h to get white powder RHA. Then, 16 g of RHA was treated with 500 mL of 10% HCl and refluxed for about 4 h at 60°C. The refluxed solution was filtered and obtained residues were washed many times with DD water until the residue is free of acid. The white residue dried at 90°C for about 5 h, then it calcinated in furnace for about 6 h at 700°C.

2.2. Preparation of Tin (IV) Oxide (SnO_2)

Tin (IV) oxide (SnO_2) was synthesized using the sol-gel method. 50 mL of 0.1 M tin chloride, and 50 mL of 0.1 M of oxalic acid were heated individually to 80°C and then hot solutions were mixed, a white precipitate was formed. The resulting solution was cooled. The residue was filtered and washed with DD water till no Cl^- ions. The precipitate was dried at 90°C. Tin (II) oxalate formed was loaded in a muffle furnace and calcinated at 800°C for about 1h.

The overall reaction of tin (II) oxalate decomposition in equation.

$$SnCl_2 + C_2H_2O_4 \quad SnO_2 + 2HCl + 2CO \qquad (1)$$

2.3. Preparation of Nanocomposite on Tin (IV) Oxide (SnO_2-SiO_2)

1 g of tin oxide and 5 g of amorphous silica 1: 5 (SnO_2:SiO_2) ratio were added in 100 mL of DD water in 250 mL of the beaker. It is stirred at a constant rate at 100°C and then completely water evaporated. The solid mass transferred in silica crucible was calcinated at 700°C for about 4 h. The following equation,

$$SnO_2 + SiO_2 \quad SnO_2–SiO_2 \qquad (2)$$

2.4. Calculation of Surface Area and Crystallite Size of SiO_2, SnO_2, and SnO_2-SiO_2 Nanocomposite

The surface area and crystallite sizes are most assumed to be important property of any material and can disclose imperative information. Therefore, this research investigated that the surface area using Sear's equation (3) and crystallite sizes was calculated by Debye Scherrer equation (4).

According to Sear's Equation,

$$A = 32.V-25 \qquad (3)$$

where, A = Surface area of samples per gram (in m^2/g)

V = volume of 0.1N NaOH required to raise the pH from 4 to 9

According to Debye Scherrer Equation,

$$D = \frac{K\lambda}{\beta\, Cos\theta} \qquad (4)$$

where, D = average particle size in nm (or) A°

λ = wavelength of X-ray A° (or) nm

K = Dimensionless shape factor (0.9)

β = FWHM (full width at half maximum of the sharp peaks)

3. RESULTS AND DISCUSSION

3.1. Determination of Surface Area and Crystallite Size of SiO2, SnO2, and SnO_2-SiO_2

The surface area is most assumed to be an important property of any material and can disclose imperative information about its adsorption properties.

Nanosilica (SiO_2), synthesized from RHA, has large surface area because carbonyl groups are the main function groups in ash. They decrease with the increasing burning temperature. This phenomenon contributes to the decrease in surface hydroxyl groups. The surface area of RHA depends on the amorphous carbon that is formed during the burning process. Finally, the most important is that the silica layer with a surface provides chemically friendly to biological systems [18]. Moreover, SnO_2-SiO_2 (173 m^2/g) nanocomposite has larger surface area than SnO_2 (113 m^2/g) due to the synthesizing processing of nanocomposite 1: 5 (SnO_2:SiO_2) ratio.

The surface areas of SiO_2, SnO_2, and SnO_2-SiO_2 were presented in Table 1. SiO_2 has the largest surface area value (212 m^2/g). It reflected that there was more contact area than SnO_2. It may be SiO_2 composite with SnO_2 had the largest pore size, pore diameter, and pore volume as literatures. This result presented that some useful mathematical equations for the quantitative determination of in-plane and across plane crystallite sizes, average numbers of SiO_2, SnO_2, and SnO_2-SiO_2 were 4 nm, 38 nm and 32 nm that calculated by Debye Scherrer equation [15]. Therefore, their average crystallite sizes were negatively related to their surface areas shown in Table 1.

3.2. SEM Analysis of SiO_2, SnO_2 and SnO_2-SiO_2

In spectrometer SEM, the surface of the specimen was analyzed by an electron beam. The morphological structure of sample (SiO_2, SnO_2 and SnO_2-SiO_2) was studied the roughness and smoothness of their surface indicated in Figures 1-3.

SEM micrographs of SiO_2 gave a highly magnified image on the surface of a material and the adsorbents surface was irregular, rough, and highly porous, indicating the possibility of its good adsorption properties in (Figure 1) which it occurs in the RHA is already a wide distribution of sizes in the nano-range, which is < 10 nm in Table 1 [19].

The SEM micrographs of Tin (IV) oxide powder (SnO_2) are a composed wormcast like structure on lumped cracked soil without aggregated particulates shown in Figure 2.

The surface morphology of SnO_2-SiO_2 composite synthesized from RHA materials in (Figure 3). It showed a few agglomerations of particles of amorphous silica with spherical in shape, whereas a compact arrangement is due to uniform sized SnO_2 NPs. which are responsible for importing irregular shapes, with the presence of some porosity which may be due to the insertion of NPs on the surface of SiO_2. Moreover, it revealed the formation of heterogeneous mixture of agglomerates, stacked flakes, rod shape, and sheet-like structure.

Table 1: Surface area and crystallite size of SiO_2, SnO_2, and SnO_2-SiO_2.

Samples	X-ray diffraction		
	Crystallite size (nm)	Crystal structure	Surface area (m^2/g)
SiO_2	4	Tetragonal	212
SnO_2	38	Tetragonal	113
SnO_2-SiO_2	32	Tetragonal	173

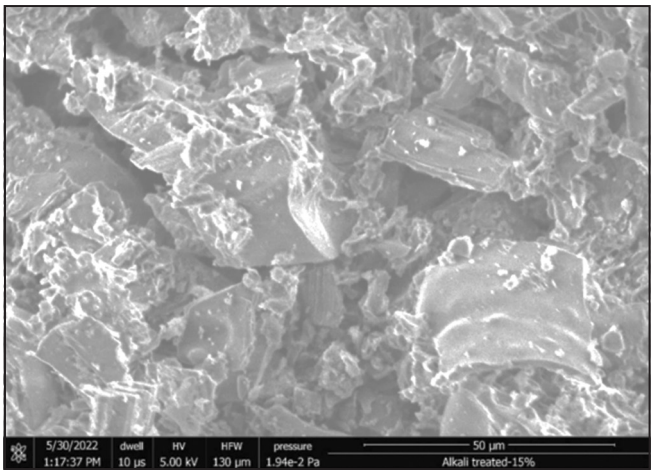

Figure 1: SEM micrograph of amorphous silica (SiO_2).

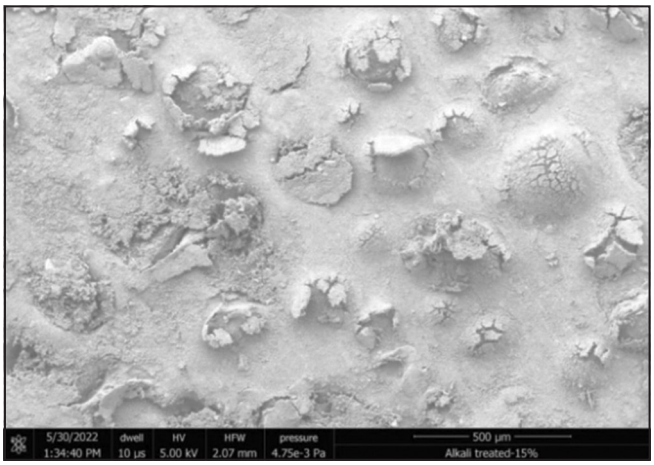

Figure 2: SEM micrograph of SnO_2.

3.3. FTIR Analysis of SiO_2, SnO_2, and SnO_2-SiO_2

3.3.1. FTIR measurement of SiO_2

FTIR spectra of SiO_2 were used to investigate the presence of functional groups in the samples from the obtained vibrational (transmittance/absorption) spectra. This analysis was based on the vibrational excitation of molecular bonds by absorption of infrared light energy within the wavelength from 3500 to 400 cm^{-1}.

To confirm the presence of SiO_2, the sample was characterized using FTIR analysis. The spectrum of the sample after calcination for 6 h at a temperature of 700°C is shown in Figure 4.

Two main characteristics peaks were observed at around 800 cm^{-1} and 1054 cm^{-1} which is attributed to the Si-O bending vibration band and asymmetric stretching vibration of the siloxane bonds (Si-O-Si). The band at about 479 cm^{-1} was associated with bending vibration modes of O-Si-O network [20].

3.3.2. FTIR measurement of SnO_2

FTIR spectra of SnO_2 were obtained in the absorption peak of 3500–400 cm^{-1} shown in Figure 5. The IR of SnO_2 contains antisymmetric vibrations of Sn–O–Sn bridge groups (663 cm^{-1}), terminal Sn–OH bonds (592 cm^{-1}), and symmetric vibrations of Sn–O (533 cm^{-1}), respectively. The strong absorption band at 632 cm^{-1} is due to the antisymmetric Sn-O-Sn vibrational mode of SnO_2 [21,22].

3.3.3. FTIR measurement of SnO_2–SiO_2

The FTIR spectrum of SnO_2-SiO_2 is shown in Figure 6. The two main characteristics peaks were observed at around 800 cm^{-1} and 1054 cm^{-1}

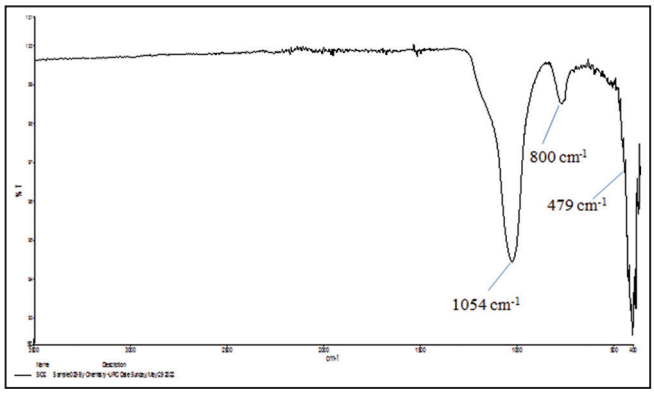

Figure 4: FTIR spectra of SiO_2.

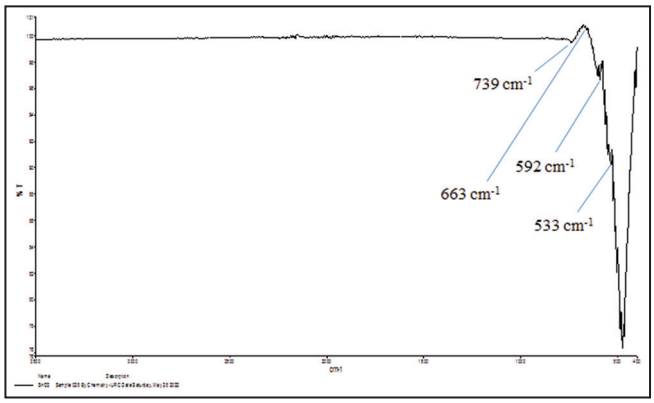

Figure 5: FTIR spectra of SnO_2.

which is attributed to Si-O bending vibration band and asymmetric stretching vibration of the siloxane bonds (Si-O-Si), respectively. The band at about 479 cm^{-1} was associated with bending vibration modes in O-Si-O network. The IR of SnO_2 contains antisymmetric vibrations of Sn-O-Sn bridge groups (663 cm^{-1}) and symmetric vibrations of Sn-O (533 cm^{-1}). The strong absorption band at 632 cm^{-1} is due to the antisymmetric Sn-O-Sn vibrational mode of SnO_2 [21]. Therefore, the absorption bands at 1054, 800, and 632 cm^{-1} are attributed to the SnO_2-SiO_2 nanocomposite [22].

3.4. XRD Analysis of SiO_2, SnO_2, and SnO_2-SiO_2

XRD was a non-destructive analytical technique which can yield the unique fingerprint of reflections associated with a crystal structure.

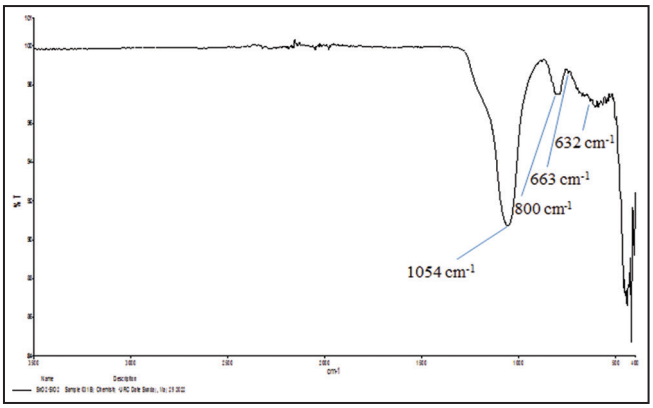

Figure 6: FTIR spectra of SnO_2–SiO_2.

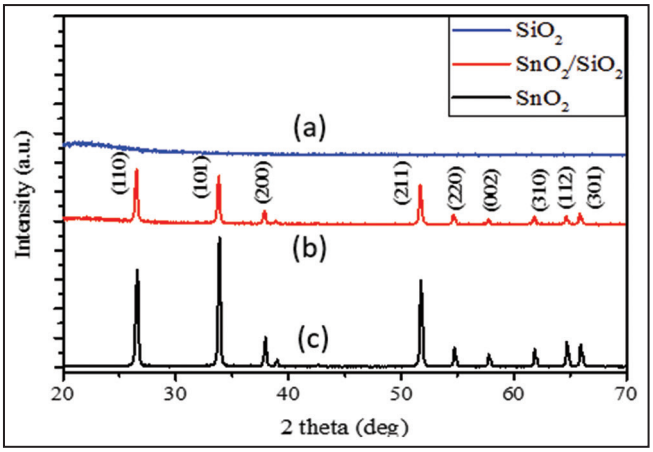

Figure 7: XRD patterns of (a) SiO_2 (b) SnO_2-SiO_2 and (c) SnO_2.

X-ray with a wavelength to the distances between these planes can be reflected such that the angle of reflection is equal to the angle of incidence. The XRD patterns of SiO_2, SnO_2, and SnO_2-SiO_2 by XRD were shown in Figure 7.

In the XRD pattern of biogenic silica shown in (Figure 7a), a broad peak at 2θ = 22.5°, which suggested RHA derived SiO_2 has an amorphous nature. The method used in SiO_2 extraction was efficient to obtain amorphous biogenic silica (SiO_2) of high purity in nanometer scale. The XRD diffractogram of SnO_2-SiO_2 nanocomposite is shown (Figure 7b). The smaller broad curve-shaped peak at 2θ = 21.7 was contributed to amorphous silica and other peaks were formed to the crystallinity of SnO_2 at approximately 2θ = 26.6°, 33.9°, and 51.8° [23]. SnO_2-SiO_2 nanocomposite behaved as a solid mixture of SiO_2 of low crystallinity and crystalline SnO_2. Therefore, RH has large amorphous biogenic SiO_2 of high purity that added to SnO_2 provides the high influence on synthesizing of SnO_2-SiO_2 nanocomposite. XRD patterns for SnO_2 showed the presence of highly crystalline and sharp intense peaks, which are in good agreement with published literature [21]. The main diffraction peaks observed for SnO_2 are centered approximately at 2θ values of 26.6° (110), 33.9° (101) and 51.8° (211), indicating the polycrystalline nature and tetragonal crystal structure of SnO_2.

3.5. UV-Visible Spectrophotometer Analysis of SiO_2, SnO_2, and SnO_2-SiO_2

Formations of NPs of SiO_2, SnO_2, and SnO_2-SiO_2 were detected by spectral analysis under UV-Vis spectrophotometer as shown in Figure 8.

The UV–visible absorption spectra of SiO_2, SnO_2, and SnO_2-SiO_2 are shown in Figure 8. The absorption maxima wavelengths (λ_{max})

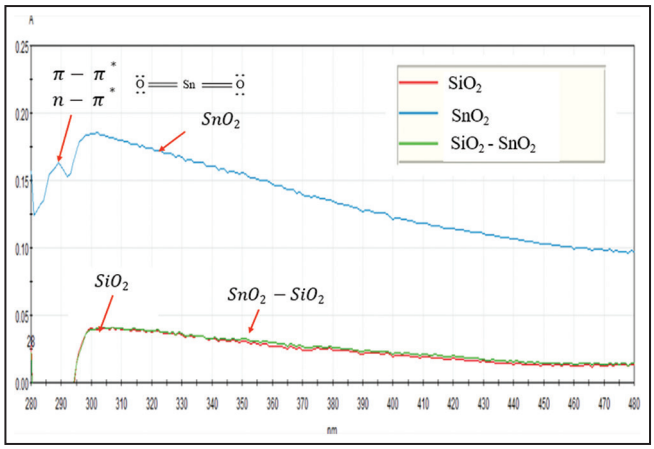

Figure 8: UV absorption spectra of SiO_2, SnO_2, and SnO_2-SiO_2.

of SnO_2 observed at 289 nm, 292 nm, and 303 nm, respectively. A strong absorption peak at 297 nm appeared corresponding to the π–π* transition and n–π* transitions of O = Sn = O in SnO_2. The absorption of SnO_2-SiO_2 has no obvious change in comparison to that pure SiO_2, indicating that strong influence of SiO_2 in synthesizing of SnO_2-SiO_2 [24].

4. CONCLUSION

Agricultural waste, RHA was applied to synthesize nanosilica (SiO_2) and tin oxide – silica nanocomposite (SnO_2-SiO_2) using sol-gel method. Resulted surface areas of SiO_2, SnO_2, and SnO_2-SiO_2 were (212, 113 and 173) m^2/g, respectively. It was found that on average crystallite size of SiO_2, SnO_2, and SnO_2-SiO_2 were 4 nm, 38 nm, and 32 nm. Therefore, their average crystallite sizes were negatively related to their surface areas. SEM results showed that the morphology of SiO_2 NPs and its nanocomposite SnO_2-SiO_2 was heterogeneous mixtures and micro-flake and irregular rod-shape particles with the aggregation of the NPs. From the FTIR spectral data, the absorption bands of SiO_2 peak at 1054 cm^{-1} for Si-O stretching vibration and 800 cm^{-1} due to the Si-O-Si bending vibrational mode. The bands for SnO_2 peaks 533 cm^{-1} and 663 cm^{-1} were assigned to the Sn-O stretching vibration and Sn-O-Sn asymmetric vibration. The absorption bands at 1054 cm^{-1}, 800 cm^{-1}, and 663 cm^{-1} are attributed to the SnO_2-SiO_2 nanocomposite. The XRD of biogenic silica showed a broad peak at 2θ = 22.5°, which suggested RHA derived SiO_2 has an amorphous nature. The main diffraction peaks observed for SnO_2 are centered approximately at 2θ values of 26.6° (110), 33.9° (101), and 51.8° (211), respectively. The XRD pattern for the nanocomposite is a small shoulder at 2θ = 21.7° that can be attributed to amorphous SiO_2 and other peaks assigned to crystalline SnO_2. As a cost-effective, easily prepared, and environmentally friendly bio-sorbents, can be applied for water treatment.

5. ACKNOWLEDGMENTS

The authors Dr Hlaing Hlaing Myint and Aung Phyo Kyawe are thankful to the Departmental Special Assistance Scheme under the University Grants Commission, and Department of Chemistry, Monywa University of Myanmar, for financial support and instrumental facilities to continue this research work.

6. REFERENCES

1. J. Umeda, K. Kondoh, Y. Michiura, (2007) Process parameters optimization in preparing high-purity amorphous silica originated from rice husks, ***Materials Transactions,* 48(12):** 3095-3100.

2. J. Shen, X. Liu, S. Zhu, H. Zhang, J. Tan, (2011) Effects of calcination parameters on the silica phase of original and leached rice husk ash, ***Materials Letters,*** **65(8):** 1179-1183.
3. I. B. Ugheoke, O. Mamat, (2012) A critical assessment and new research directions of rice husk silica processing methods and properties, *Maejo* ***International Journal of Science and Technology,*** **6(3):** 430-448.
4. E. M. Ginting, B. Wirjo-Sentono, N. Bukit, H. Agusnar, (2014) Preparation and characterization of rice husk ash as filler material in to nanoparticles on Hdpe thermoplastic composites, ***Chemistry and Materials Research,*** **6(7):** 2224-3224.
5. A. A. Yelwande, M. E. Navgire, D. T. Tayde, B. R. Arbad, M. K. Lande, (2012) SnO_2/SiO_2 nanocomposite catalyzed one-pot synthesis of 2-arylbenzothiazole derivatives, ***Bulletin of the Korean Chemical Society,*** **33(6):** 1856-1860.
6. L. Sun, K. Gong, (2001) Review, silicon-based materials from rice husks and their applications, ***Industrial and Engineering Chemistry Research,*** **40:** 5861-5877.
7. S. M. A. Francis, V. Thiruvengadam, (2020) Catalytic reduction of rhodamine B and crystal violet using SnO_2-SiO_2 nanocomposite derived from rice husk, ***International Research Journal of Engineering and Technology (IRJET)***, **7(12):** 2395-0072**.**
8. A. Chavez-Calderon, F. Paraguay-Delgado, E. Orrantia-Borunda, A. Luna-Velasco, (2016) Size effect of SnO_2 nanoparticles on bacteria toxicity and their membrane damage, ***Chemosphere,*** **165:** 33-40.
9. D. Skoda, A. Styskalik, Z. Moravec, P. Bezdicka, J. Bursik, P. H. Mutin, J. Pinkas, (2016) Mesoporous SnO_2-SiO_2 and Sn-silica-carbon nanocomposites by novel non-hydrolytic templated sol-gel synthesis, ***The Royal Society of Chemistry,*** **6:** 68739-68747.
10. P. Sharma, R. Kaur, C. Baskar, W. J. Chung, (2010) Removal of methylene blue from aqueous waste using rice husk and rice husk ash, ***Desalination*****, 259(1-3):** 249-257.
11. L. Dong, W. Linghu, D. Zhao, Y. Mou, B. Hu, A. M. Asiri, K. A. Alamry, D. Xu, J. Wang, (2018) Performance of biochar derived from rice straw for removal of Ni (II) in batch experiments, ***Water Science and Technology*****, 2017(3):** 824-834.
12. U. Kalapathy, A. Proctor, J. Shultz, (2002) An improved method for production of silica from rice hull ash, ***Bioresource Technology,*** **85(3):** 285-289.
13. R. Supitcha, P. Wachira, S. Natthapong, (2009) Preparation of silica gel from rice husk using microwave heating, ***Journal of Metals, Materials, and Mineral,*** **19(2):** 45-50.
14. G. Sears, (1956) Determination of specific surface area of colloidal silica by titration with sodium hydroxide, ***Analytical Chemistry,*** **28:** 1981-1983.
15. P. Scherrer, (1918) Determination of the size and the internal structure of Colloidal Particles by X-rays, ***Mathematical Physics Class*****, 1918:** 98-100.
16. J. I. Langford, A. J. C. Wilson, (1978) Scherrer after sixty years: A survey and some new results in the determination of crystal lite size, ***Journal of Applied Crystallography,*** **11:** 102-113.
17. H. Riveros, C. Garza, (1986), Rice husk as a source of high purity silica, ***Journal of Crystals Growth,*** **75(1):** 126-113.
18. W. A. P. J. Premaratne, W. M. G. I. Priyadarshana, S. H. P. Gunawardena, A. A. P. De Alwis, (2014) Synthesis of nanosilica from paddy husk ash and their surface functionalization, ***Journal of Science of the University of Kelaniya Sri Lanka,*** **8**, 33-48.
19. Z. A. A. Halim, M. A. M. Yajid, M. H. Idris, H. Hamdan, (2018) Effects of rice husk derived amorphous silica on the thermal-mechanical properties of unsaturated polyester composites, ***Journal of Macromolecular Science,*** **57(6):** 479-496.
20. R. A. Bakar, R. Yahya, S. N. Gan, (2016), Production of high purity amorphous silica from rice husk, ***Procedia Chemistry,*** **19:** 189-195.
21. D. Gulevich, M. Rumyantseva, E. Gerasimov, A. Marikutsa, V. Krivetskiy, T. Shatalova, N. Khmelevsky, A. Gaskov, (2019) Nanocomposites SnO_2/SiO_2 for CO gas sensors: Microstructure and reactivity in the interaction with the gas phase, ***Materials,*** **12:** 1096.
22. A. A. Yelwande, M. K. Lande**, (**2018**)** Synthesis and characterization of SnO_2/SiO_2 nanocomposite catalytic material, ***International Journal of Engineering Technology Science and Research, IJETSR,*** **5(1):** 2394-3386.
23. C. S Ferreira, P. L Santos, J. A Bonacin, R. R Passos, L. A Pocrifka, (2015) Rice husk reuse in the preparation of SnO2/SiO2 nanocomposite, Materials Research, **18(3):** 639-643.
24. Y. Lei, X. Bing, Z. Zhang, C. Fang, (2017) Solvothermal synthesis of SnO2/grapheme composites with improved photoelectric photoelectric characteristics, ***Journal of Materials Science: Materials in Electronics,*** **28:** 17058-17062.

****Bibliographical Sketch***

Dr. Hlaing Hlaing Myint is an Associate Professor, Department of Chemistry, Monywa University, Myanmar. Her Doctor of Engineering (D.Eng:) graduated from Department of Transdisciplinary Science and Engineering, Tokyo Institute of Technology (TIT) Japan under the supervision of Prof. Jeffrey S. Cross in 2015. And also, her Post-doctoral Research Fellowship received under the guidance of Prof. Dr. K.S.V. Krishna Rao, Department of Chemistry, Yogi Vemana University, India. Her research interests are in the areas of Chemical engineering, Ionic Liquids, Adsorption Isotherm, Wastewater Treatment, Nanocomposite, Graphene Oxide, Magnetite nanoparticles (Fe3O4) and Synthesis of Hydrogel. She wrote Abstract book [One book chapter, 2017]. She served as an International Advisory Committee at Thai Institute of Chemical Engineering and Applied Chemistry (TIChE) in 2018. She attended many regional seminars and International Conferences for presenting her research work at Japan 2014, China, 2014, South Korea, 2018, Indonesia 2018, Vietnam 2019, India 2022.

Mr. Aung Phyo Kywae, Demonstrator, Department of Chemistry, Shwebo University, Myanmar. He obtained B.Sc Qualifying Biochemistry from Monywa University in 2018. He completed M.Sc degree under the supervision of Dr. Hlaing Hlaing Myint, Associate Professor, Department of Chemistry, Monywa University, Myanmar in 2022.